Adsorption and catalytic combustion of ARB on CuO-Fe$_2$O$_3$

WU Rongcheng, QU Jiuhui, HE Hong & YU Yunbo

Research Center for Eco-Environmental Sciences, Chinese Academy of Sciences, Beijing 100085, China
Correspondence should be addressed to Qu Jiuhui (e-mail: jhqu@ mail.rcees.ac.cn)

Abstract   CuO-Fe$_2$O$_3$ composite material with strong magnetism and a large surface area is prepared by the co-precipitate method. Its adsorption properties towards Acid Red B (ARB) and the regeneration by catalytic combustion of organic compounds have been studied. The results show that the prepared CuO-Fe$_2$O$_3$ composite is an excellent adsorbent for ARB adsorption at acid condition. The presence of Cl$^-$ has no effect on ARB adsorption. But the SO$_4^{2-}$ can inhibit ARB adsorption. After being recovered by the magnetic separation method, the adsorbent can be regenerated by catalytic oxidation of absorbate at 300℃ in air atmosphere. The combustion reactions of ARB in the presence or absence of CuO-Fe$_2$O$_3$ are studied by *in situ* diffuse reflection FTIR. The results indicate that, in the presence of CuO-Fe$_2$O$_3$, the degradation temperature is significantly lowered by the catalysis of CuO-Fe$_2$O$_3$, and ARB can be oxidized completely without volatile organic compound by-product; in comparison, in the absence of CuO-Fe$_2$O$_3$, the temperature needed for oxidation of ARB is higher and the reaction is incomplete with some N-containing harmful compounds produced. The reusability of CuO-Fe$_2$O$_3$ is also studied in successive seven adsorption-regeneration cycles.

Keywords: CuO-Fe$_2$O$_3$, Acid Red B, adsorption, catalytic combustion, *In situ* FTIR.

Some organic contaminants, such as dyes, are toxic and non-biodegradable and cannot be efficiently removed from water by common biological, physical or chemical processes. Activated carbon powder can be used to remove efficiently those organic contaminants with the advantages of high adsorption rate and large adsorption capacity owing to its small particle size, large surface area and good dispersion in water. But the cost is high because of difficulties of separation and reuse.

The uses of clays or metal oxides as adsorbents or catalysts for the removal of pollutants from water have been the subject of several recent studies[1—5]. In some of these studies, they are used in the form of powders, which leads to a larger contacting area with aqueous phase and thus a faster adsorption rate and a higher adsorption capacity. But their application is also limited by the difficulties of separation and regeneration. Copper oxide and iron oxides are conventional catalysts and have shown good adsorption properties and catalytic oxidation activity towards some organic compounds. It is known that the composite of copper oxide and iron oxide —CuFe$_2$O$_4$ is magnetic and can be recovered efficiently by the magnetic separation method. Thus, the use of copper oxide and iron oxide composite as adsorbent/catalyst for the removal of organic contaminants may overcome the recovery and regeneration difficulties in water treatment. However, little work has been done on this subject in literature at present. The aim of this work is to evaluate the effectiveness of powder CuO-Fe$_2$O$_3$ composite as adsorbent/catalyst for the removal of azo dye Acid Red B (ARB), as a model compound, by adsorption-catalytic combustion. In this study, powder CuO-Fe$_2$O$_3$ composite with strong magnetism and large surface area is prepared by the co-precipitate method, the properties of adsorption and regeneration have been studied, the reaction mechanism of ARB in the presence and absence of CuO-Fe$_2$O$_3$ composite is also studied by *in situ* diffusion reflection FTIR.

1   Experimental

（ⅰ）Materials. CuO-Fe$_2$O$_3$ was prepared by the co-precipitation method. 0.03 mol Cu(NO$_3$)$_2$ • 3H$_2$O and 0.06 mol Fe(NO$_3$)$_3$ • 9H$_2$O was dissolved in 100 mL of distilled water. Under vigorous magnetic-stirring the pH was slowly raised by adding 3 mol/L NaOH solution to around 10 and stirring continued for 30 min, and then stopped. The suspension was heated to 100℃ and kept for 4 h. After cooling, the pH of solution was adjusted to about 7 by adding 0.2 mol/L HCl. Then the prepared magnetic adsorbent was repeatedly washed with distilled water. By magnetic separation, the solid was separated from water, and then dried at 50℃ and 110℃ for 8 h respectively. The dry material was crushed and stored for further tests. Its specific saturation magnetization (σ_s) of 20.42 emu/g was determined using a VSM model 155 magnetic meter. The BET area was measured to be 86 m^2/g. The average particle size determined by Mastersizer 2000 (Malvern Co) is 14.2 µm. The XRD pattern revealed the spinel structure of CuFe$_2$O$_4$.

Acid Red B was purchased from Beijing Chemicals Co (Beijing, China) and used without further purification. Its structure is:
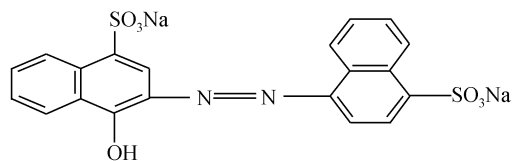
Deionized water was used throughout this study.

（ⅱ）Methods. For all adsorption experiments, the suspension containing 0.200 g adsorbent and varying

amount of ARB was shaken on an orbit shaker at 140 r/min. The temperature was controlled at 25℃ by air bath. The pH was adjusted by addition of HCl or NaOH. The adsorption time was 2 h. The concentration of ARB was determined by spectrophotometer (U-3010, Hitachi Co) at 516 nm or by TOC analyzer (Phoenix 8000, Tekmar Dohrmann Co, USA) after 0.45 μm membrane filtration.

For the experiments of effect of pH on adsorption, 50 mL, 100 mg/L ARB solution was used. Adsorption isotherm was conducted using the completely mixed batch reactor bottle-point method, and the solution pH was at 4.0. For the test of influence of inorganic anions on ARB removal efficiency, 100 mg/L ARB solutions containing 0.0010, 0.010 and 0.10 mol/L NaCl or Na_2SO_4 were used, respectively.

After adsorption, the adsorbent was recovered by the magnetic separation method with a permanent magnet of 40 mm diameter and 10 mm thickness, made with Nd-Fe-B (2300 Gauss).

The regeneration of $CuO-Fe_2O_3$ via thermal degradation of adsorbate was carried out with the following processes: After magnetic separation, the collected adsorbent loaded with ARB was dried at 100℃, then placed into a muffle furnace and heated at 300℃ for 30 min, the air was let in at a flow of 100 mL/min. After reaction, the regenerated $CuO-Fe_2O_3$ was washed with 10 mL NaOH solution of pH 8─9 for further tests.

Diffuse reflection IR spectra of the combustion of ARB and ARB adsorbed on $CuO-Fe_2O_3$ was determined by a Nicolet 670 FTIR spectrophotometer, equipped with a controlled-temperature and environment diffuse reflectance *in situ* chamber and a liquid nitrogen-cooled Hg-CdTe detector. The air was let in at a flow of 100 mL/min.

2 Results and discussion

(ⅰ) Effectiveness of ARB adsorption by $CuO-Fe_2O_3$

(1) ARB removal efficiency at various pH. The effect of solution pH on adsorption varies significantly with different adsorbent or adsorbate. Fig. 1 shows the removal of ARB by $CuO-Fe_2O_3$ at various pH. 50 mL ARB solution at the initial dye concentration of 100 mg/L was used. It indicates that the removal efficiency is strongly dependent on pH. Acidic condition is favorable for the removal of ARB, especially at pH<5, the removal efficiency of ARB is very high. At pH >5, the effectiveness of removal for ARB decreases drastically with the pH increaseing.

In the reaction of adsorption, the charges of adsorbent and adsorbate played an important role. Heterocharge of adsorbent and adsorbate is in favor of adsorbing reaction. From the literature value $pK_{a_1} \approx 1$ for the ─SO_3H group and pK_{a_2} value of 11.4 for the naphthalene ─OH of Orange Ⅱ[6], an azo dye with the similar structure to ARB, it could be deduced that at the pH range studied,
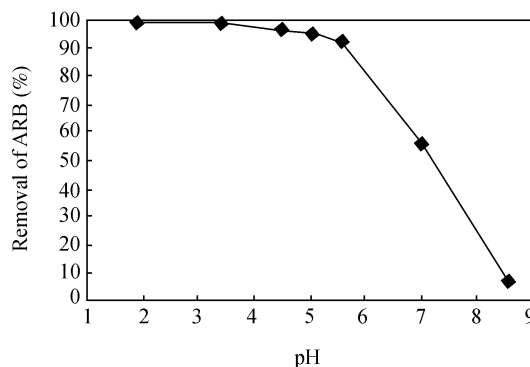

Fig. 1. Effect of pH on removal efficiency. 50 mL ARB solution, initial concentration 100 mg/L, pH 4.8; 0.100 g $CuO-Fe_2O_3$.

most of ARB existed as HA^{2-}, the fraction of other forms was at negligible level. Thus, it was mainly controlled by the charges of adsorbent surface when interactions between ARB and adsorbent varied with the pH of solution. At lower pH more protons were available to protonate oxides surface of adsorbents, thereby increased electrostatic attractions between negatively charged dye molecules and positively charged oxides surface of adsorbents, which was in favor of adsorption reaction. While at higher pH, the adsorbent surface decreased in positive charges or even negative charges, which did not favor the adsorption. So adsorption of ARB by $CuO-Fe_2O_3$ should be performed at acid conditions which is in accordance with the pH of actual dye wastewater.

(2) Adsorption isotherm. Adsorption capacity at different aqueous equilibrium concentration can be illustrated by the adsorption isotherm. Fig. 2 shows the adsorption isotherm of ARB on $CuO-Fe_2O_3$ at pH 4.0 and 25℃.
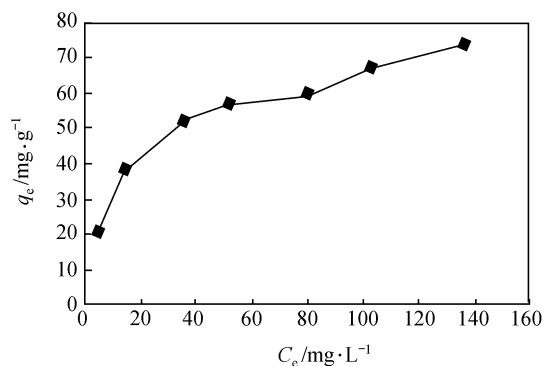

Fig. 2. Adsorption isotherm of ARB on $CuO-Fe_2O_3$ at pH 4.0.

Langmuir and Freundlich adsorption models were used to describe the sorption data.

Langmuir equation: $q_e = q_m b C_e/(1+b C_e)$,

Freundlich equation: $q_e = k C_e^{1/n}$,

where q_e (mg dye/g adsorbent) is the amount of dye ad-

sorbed per gram of adsorbent at equilibrium; q_m (mg dye/g adsorbent) is the maximum adsorption capacity; C_e (mg/L) is the equilibrium concentration of dye in solution.

The correlation coefficient $R_L^2 = 0.99$ for Langmuir model and $R_F^2 = 0.95$ for Freundlich model indicated that Langmuir model was more appropriate than that of Freundlich model. The calculated maximum adsorption capacity q_m of ARB on CuO-Fe$_2$O$_3$ at pH 4.0 is 74.1 mg/g.

(3) Effect of inorganic anions on ARB adsorption. Inorganic salts are often present in effluent and they may affect adsorption in some case. Cl$^-$ and SO$_4^{2-}$ are commoly co-existing anions as well as dyes in wastewater. The effect of Cl$^-$ and SO$_4^{2-}$ on ARB removal by CuO-Fe$_2$O$_3$ adsorbent is shown in Table 1. It can be seen that there was no effect on ARB removal in the presence of Cl$^-$ at the concentration range of 0—0.1 mol $\cdot$ L^{-1} Cl$^-$. But the effect of SO$_4^{2-}$ on the removal of ARB was very significant. In the presence of SO$_4^{2-}$ at 0.0010 mol $\cdot$ L^{-1}, the removal of ARB dropped from 96% to about 85%; at concentration of 0.010 mol $\cdot$ L^{-1} SO$_4^{2-}$, the removal of ARB dropped to 32.5%, and that at the concentration of 0.10 mol/L SO$_4^{2-}$, the removal of ARB dropped to about 18%.

Table 1　Effect of inorganic anions on ARB adsorption[a]

Anion	Concentration of anion/mol $\cdot$ L^{-1}	ARB removal (%)
Cl$^-$	0.0010	95.8
	0.010	96.1
	0.10	95.2
SO$_4^{2-}$	0.0010	85.2
	0.010	32.5
	0.10	18.1

a) CuO-Fe$_2$O$_3$: 0.200 g; ARB solution: 100 mg/L, 50 mL; pH=4.

The results of this test indicate the competition of SO$_4^{2-}$ with ARB for active site on CuO-Fe$_2$O$_3$ that did not exist between Cl$^-$ and ARB. This could be attributed to the chemisorption of ARB on CuO-Fe$_2$O$_3$ via $-$SO$_3^-$ of the dye through the formation of complex with the adsorbent surface as studied by FTIR later. SO$_4^{2-}$ has the similar structure to $-$SO$_3^-$, thus it could also have chemisorption on CuO-Fe$_2$O$_3$ and decreased ARB adsorption.

(4) FTIR spectra for ARB adsorption on CuO-Fe$_2$O$_3$. The FTIR spectra of ARB, adsorbed ARB on CuO-Fe$_2$O$_3$ and initial CuO-Fe$_2$O$_3$ are shown in Fig. 3. The peaks at 1603 and 1501 cm^{-1} are assigned to aromatic C=C stretching vibration[6], while the weak peak at 1463 cm^{-1}

corresponds to $-$N=N$-$ bond stretching vibration, and the peaks at 1207, 1436 cm^{-1} are assigned to $-$C-O$-$ bond stretching vibration and $-$OH deformation, respectively. The $-$SO$_3^-$ asymmetric vibration is shown at 1277 cm^{-1} and its symmetric overlaps with $-$C-O$-$ bond stretching vibration at about 1200 cm$^{-1[6]}$. It can be seen that peaks of adsorbed ARB on CuO-Fe$_2$O$_3$ were similar to those of ARB except for the peaks at 1436 cm^{-1} ($-$OH) and 1277 cm^{-1} ($-$SO$_3^-$) that almost disappeared after adsorption, and the peak at 1200 cm^{-1} also changed obviously. This suggests the participation of both $-$C-OH and $-$SO$_3^-$ groups in bond formation with the adsorbent surface and confirms the chemisorption of ARB on CuO-Fe$_2$O$_3$.
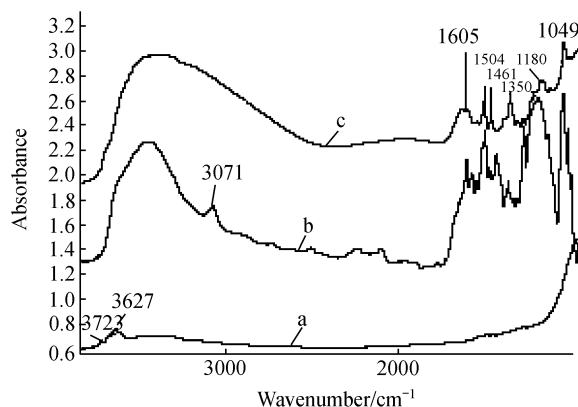

Fig. 3.　FTIR spectra for ARB adsorption on CuO-Fe$_2$O$_3$. a, CuO-Fe$_2$O$_3$; b, ARB; c, ARB adsorbed on CuO-Fe$_2$O$_3$.

(ⅱ) Catalytic combustion of ARB and regeneration of CuO-Fe$_2$O$_3$

(1) The reusability of CuO-Fe$_2$O$_3$ regenerated by catalytic combustion of organic compounds. Seven adsorption-combustion cycles were carried out to evaluate the reusability of CuO-Fe$_2$O$_3$ as adsorbent/catalyst for the removal of ARB. Fig. 4 shows the removal efficiency of ARB during the seven cycles, for 50 mL ARB solution of initial concentration 100 mg $\cdot$ L^{-1} at pH 4. CuO-Fe$_2$O$_3$ was washed after each combustion using a NaOH solution of pH 8—9 for the removal of nitrate or sulfate formed in the oxidation reaction. The results demonstrated that the removal efficiency only decreased slightly after the first cycle, and then it reached a stable state in the following cycles. These experiments demonstrated that CuO-Fe$_2$O$_3$ as adsorbent/catalyst could be used repeatedly over many cycles.

(2) Catalytic combustion of ARB on CuO-Fe$_2$O$_3$. In order to obtain insights into the reaction process, combustion of ARB in the presence or absence of CuO-Fe$_2$O$_3$ was studied by means of in situ DRIFT spectroscopy. In the
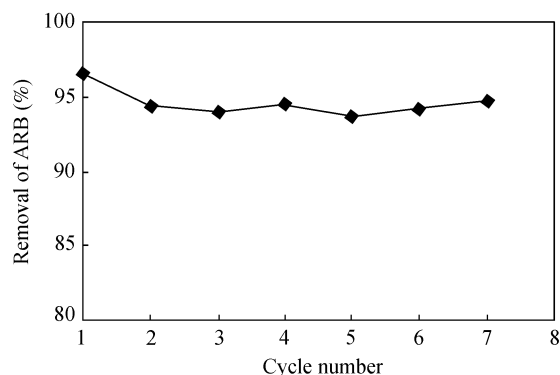
Fig. 4. The removal efficiency of ARB during seven cycles, for 50 mL ARB solution of initial concentration 100 mg·L^{-1} at pH 4.0.

test, 10 mg ARB (by itself diluted by KBr or adsorbed on CuO-Fe$_2$O$_3$) were placed into the *in situ* reactor, and the air was let in at a flow of 100 mL/min. The infrared spectra of the combustion at different temperatures are shown in Figs. 5 and 6.

Fig. 5 shows the combustion reaction of ARB at 150℃, 200℃ and 250℃ in the presence of CuO-Fe$_2$O$_3$. It can be seen that at 150℃, the spectra already changed evidently: the peak at 1048 cm^{-1} and the peaks between 1100—1250 cm^{-1} (—SO$_3^-$ and —C-OH) decreased obviously, and the peak at 1461 cm^{-1} (—N=N—) decreased slightly. A new peak at 1581 cm^{-1} (R—NO) appeared. The peaks (1605 and 1504 cm^{-1}) corresponding to aromatic ring vibrations showed no change at 150℃. This indicated that the oxidation of sulfonic group (—SO$_3^-$) was the main reaction for ARB on CuO-Fe$_2$O$_3$ at 150℃, and the azo bond also reacted slowly, while aromatic ring was stable at this temperature. At 200℃, the change in spectra was more drastic: The peaks between 1100—1250 cm^{-1} (—SO$_3^-$ and —C—O) and 1461 cm^{-1} (—N=N—) disappeared or were very weak, while the peak at 1581 cm^{-1} (R—NO) increased rapidly and a new peak at 1551 cm^{-1} (—NO$_2$) appeared. This indicated that the rapid oxidation of —N=N— to nitro-compounds and the further oxidation of —SO$_3^-$ and —C-OH had taken place. At 250℃, the peaks between 1100—1250 cm^{-1} (—SO$_3^-$ and —C-O) and 1463 cm^{-1} (—N=N—) almost disappeared and the peak at 1551 cm^{-1} (—NO$_2$) increased rapidly. And the nitrate peak at 1330 cm^{-1} appeared. These results indicated that the reactions of ARB in the presence of CuO-Fe$_2$O$_3$ below 250℃ were mainly of the oxidation of —SO$_3^-$, —C-OH and —N=N—.

At 300℃ (as shown in Fig. 6), the peaks between 1500—1600 cm^{-1} (C=C, and —NO$_2$) decreased drastically, and the peaks at 1338 cm^{-1} (NO$_3^-$), 2321—2370 cm^{-1} (CO$_2$) appeared rapidly at the same time, which confirmed that the fast oxidation of aryl and —NO$_2$ to CO$_2$ and nitrate had taken place, respectively. After 10 min, only the peak at 1338 cm^{-1} (NO$_3^-$) was obvious. This indicated the complete oxidation of ARB. And no volatile organic compound detected by MS on line during the reaction also demonstrated the complete oxidation of ARB in the presence of CuO-Fe$_2$O$_3$. It is also indicated in Fig. 6 that the surface of CuO-Fe$_2$O$_3$ after regeneration was similar to that of the initial one except nitrate left. While nitrate could be washed out or dissolved during the next adsorption cycle, thus having no effect on the adsorption-regeneration performance. This was consistent with the test results as stated previously.

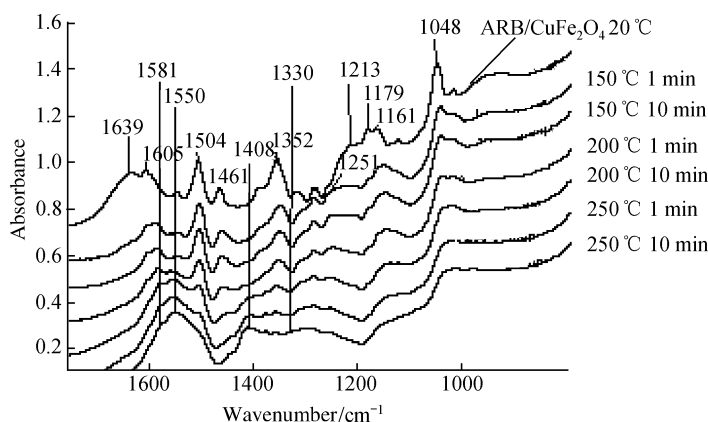From these results, a reaction scheme for ARB combustion on CuO-Fe$_2$O$_3$ at different temperatures is given:

Fig. 5. FTIR spectra for ARB/ CuO-Fe$_2$O$_3$ combustion at 150℃, 200℃ and 250℃.

$$\text{Heating } 150\,^\circ\text{C} \quad -\text{OH}, -\text{SO}_3^- \xrightarrow{[O]} \text{H}_2\text{O}, \text{SO}_2\,;$$

$$\text{Air} \quad 200-250\,^\circ\text{C} \quad -\text{N}=\text{N}- \xrightarrow{[O]} \text{R}-\text{NO}_2,\ \text{R}-\text{NO and NO}_3^-\,;$$

$$300\,^\circ\text{C} \quad -\text{Ar}, \text{R}-\text{NO}_2, \xrightarrow{[O]} \text{R}-\text{NO}, \text{CO}_2, \text{H}_2\text{O}, \text{NO}_3^-$$
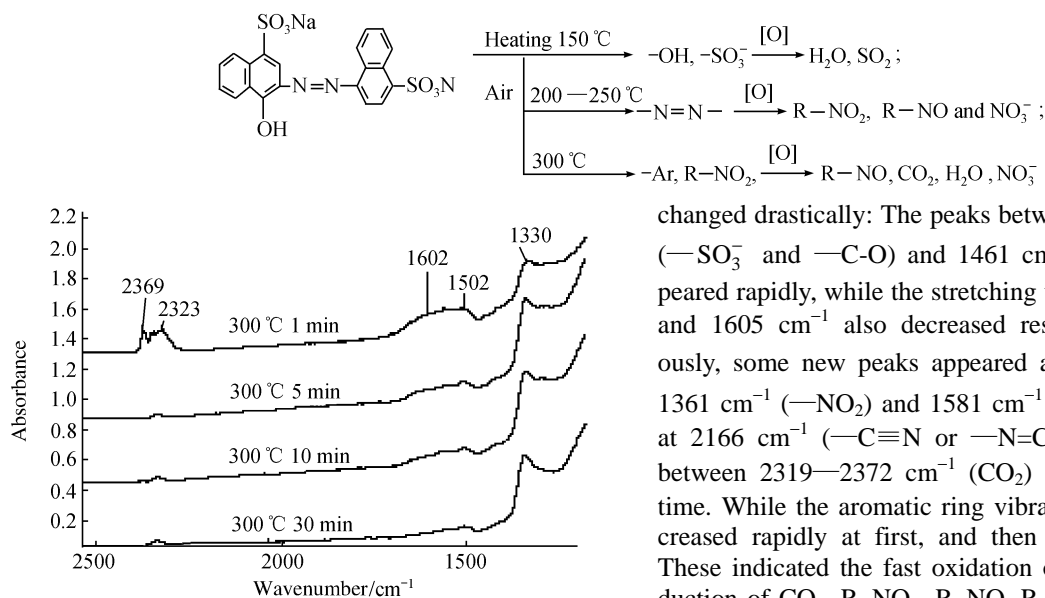
Fig. 6.   FTIR spectra for ARB/CuO-Fe$_2$O$_3$ combustion at 300 ℃

(iii) The catalysis of CuO-Fe$_2$O$_3$ in ARB combustion. For comparing the oxidation processes of ARB under different conditions, the reaction of ARB in the absence of CuO-Fe$_2$O$_3$ was also studied. Fig. 7 shows the changes of IR spectra for ARB oxidation in air atmosphere in the absence of CuO-Fe$_2$O$_3$. In the absence of CuO-Fe$_2$O$_3$, the IR spectra show no obvious change at the temperature below 300 ℃, except for the disappearing of the peak at 1640 cm^{-1} (H$_2$O). This indi cates that ARB was stable at this temperature.

When the temperature rose to 500 ℃, the spectra changed drastically: The peaks between 1100—1250 cm^{-1} (—SO$_3^-$ and —C-O) and 1461 cm^{-1} (—N=N—) disappeared rapidly, while the stretching vibration C=C at 1504 and 1605 cm^{-1} also decreased respectively. Simultaneously, some new peaks appeared at 1111 cm^{-1} (SO$_4^{2-}$), 1361 cm^{-1} (—NO$_2$) and 1581 cm^{-1} (—NO)[7,8]. The peak at 2166 cm^{-1} (—C≡N or —N=C=O)[9] and the peaks between 2319—2372 cm^{-1} (CO$_2$) appeared at the same time. While the aromatic ring vibration at 1504 cm^{-1} decreased rapidly at first, and then slowly 10 min later. These indicated the fast oxidation of ARB with the production of CO$_2$, R—NO$_2$, R—NO, R—C≡N and R—N=C=O. But the aromatic ring was not completely oxidized. After 40 min, the peaks at 1361 cm^{-1} (—NO$_2$) and 1207 cm^{-1} (C—O) disappeared, the peak at 2166 cm^{-1} (—C≡N or —N=C=O) and the peaks between 1500—1600 cm^{-1} (C=C) decreased, but did not disappear. Even at 600 ℃ and after being reacted for 20 min, the peaks between 1500—1600 cm^{-1} still remained. The results indicated that at 500 ℃ all groups of ARB molecules were oxidized, but the oxidation was not complete.

From the changes of the peaks at 2166, 1581 and 1361 cm^{-1} that increased at first and decreased at later, it can be deduced that the amount of the corresponding
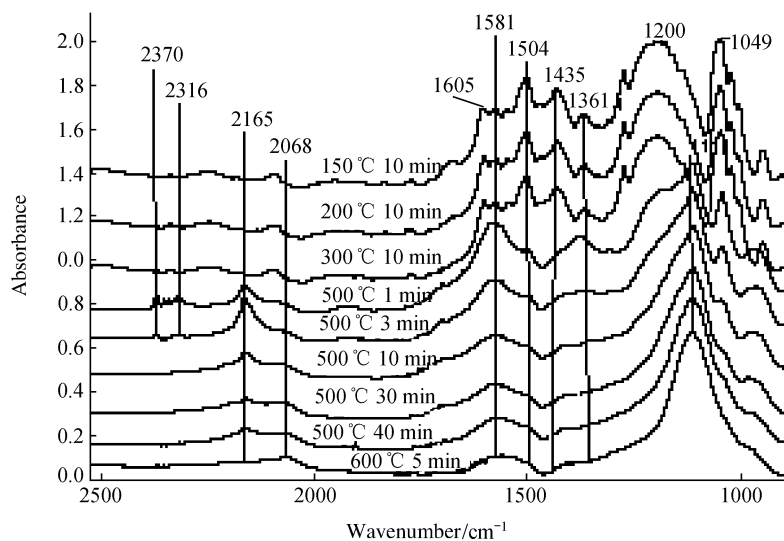
Fig. 7.   FTIR spectra for ARB combustion at different temperature.

N-containing compounds R–C≡N, R–NO and R–NO₂ also increased at first and then decreased instead of accumulation. But it is noted that there was no nitrate peak (1300—1400 cm⁻¹) appeared. This implied the volatilization of the N-containing compounds mentioned above or their decomposition to other products instead of producing nitrate.
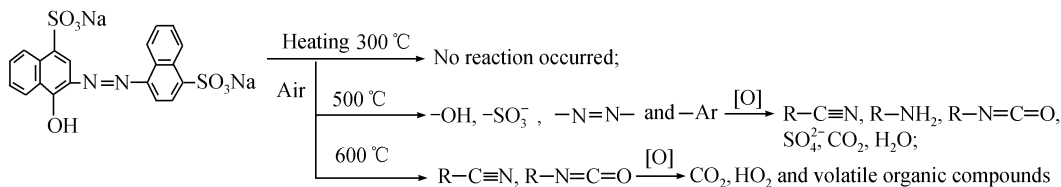
By comparing Fig. 7 with Figs. 5 and 6, the difference of the reactions of ARB under both conditions was clearly shown: firstly, the temperature needed for reaction was different. A higher temperature (500℃) was needed in the absence of CuO-Fe₂O₃ for ARB oxidation compared with that of in the presence of CuO-Fe₂O₃ (150℃). Secondly, the intermediate and the final products are also different. In the absence of CuO-Fe₂O₃, the strongest peak in IR spectra was at 1581cm⁻¹ in the range of 1500—1600 cm⁻¹ during the reaction, no nitrate but sulfate peak appeared. The combustion was not complete even at 600℃, and some volatile N-containing organic compounds were generated. Comparatively, in the presence of CuO-Fe₂O₃, the strongest peak was at 1550 cm⁻¹ in the range of 1500—1600 cm⁻¹ during the reaction. Obvious nitrate peak appeared instead of sulfate peak. No organic compound was found in the volatile products and on the adsorbent after combustion, which indicated the complete oxidation of ARB.

It can be concluded from the experiments for the combustion of ARB in the presence or absence of CuO-Fe₂O₃ that the CuO-Fe₂O₃ composite has excellent catalytic activity towards ARB combustion. It not only lowered the temperature required for reaction but also achieved the complete oxidation of ARB to CO_2, H_2O and nitrate.

3 Conclusions

Firstly, the prepared magnetic CuO-Fe₂O₃ powder is proven to possess excellent adsorptive properties towards azo dye ARB. Chemisorption is of the main adsorption mechanism through the participation of — SO_3^- and —C-OH group of ARB in bond formation with the adsorbent surface. After adsorption, it can be conveniently recovered by magnetic separation technology.

Secondly, the CuO-Fe₂O₃ adsorbent can be regenerated by complete combustion of the adsorbed dye. The properties of CuO-Fe₂O₃ were stable during seven adsorption-combustion cycles.

Thirdly, the CuO-Fe₂O₃ powder has high catalytic

The volatile N-containing compounds such as nitrile and amines were indeed detected by MS during the combustion.

From this study, a reaction scheme for ARB combustion in the absence of CuO-Fe₂O₃ at different temperatures can be given:

activity towards ARB combustion. The oxidation reaction is complete and could be carried out at relatively low temperature with no organic product emitted to atmosphere or deposited on the CuO-Fe₂O₃ surface after ARB combustion.

References

1. Gu, B., Schmitt, J., Chen, Z. et al., Adsorption and desorption of natural organic matter on iron oxide: mechanisms and model, Environ. Sci. Technol., 1994, 28: 38—46.

2. Heijman, S. G. J., Paassen, A. M., Meer, W. G. J. et al., Adsorptive removal of natural organic matter during drinking water treatment, Wat. Sci. Technol., 1999, 40(9): 183—190.

3. Herrera, F., Lopez, A., Mascolo, G. et al., Catalytic combustion of Orange II on hematite: surface species responsible for the dye degradation, Applied Catalysis B: Environ, 2001, 29: 147—162.

4. Gonzalez-Pradas, E., Socias-Viciana, M., Saifi, M. et al., Adsorption of atrazine from aqueous solution on heat treated kerolites, Chemosphere, 2003, 51: 85—93.

5. Zhang, Y., Yang, M., Gao, Y. X. et al., Preparation and adsorption mechanism of rare earth-doped adsorbent for arsenic (V) removal from groundwater, Science in China, Series B, 2003, 46(3): 252—258.

6. Bandara, J., Mielczarski, J. A., Kiwi, J., Molecular Mechanism of surface recognition, Azo dyes degradation on Fe, Ti, and Al Oxides through metal sulfonate complexes, Langmuir., 1999, 15(22): 7670—7679.

7. Koji Nakanshi, Solomon, P. H., Infrared Absorption Spectroscopy. San Francisco: Holden-Day. Inc, 1977, 37.

8. Department of Chemistry, Hangzhou University, Handbook of Analysis Chem., Part Ⅲ (in Chinese), Beijing: Chemical Industry Press, 1983, 614.

9. Silverstein, R. M., Bassler, G. C., Morrill, T. C. (Translated by Yao Haiwen, Ma Jinshi, Huang Junxiong et al.), Spectrometric Identification of Organic Compounds, London: John Wiley, 1974, 98.